

ANALYSIS OF COMBINED HEAT AND MASS TRANSFER OF WATER-VAPOR IN A CYLINDRICAL ZEOLITE ADSORBER

Ababayehu Assefa
Mechanical Engineering Department

ABSTRACT

In this paper, the combined heat and mass transfer of water-vapor into a cylindrical zeolite adsorber has been numerically simulated. The two-dimensional heat and mass transfer equations are numerically solved using gPROMS program – a general Process Modeling System [1] program, inserting the proper initial and boundary conditions to the model. The centered finite-difference method (CFDM) approximation is employed in solving the two-dimensional partial differential equations. The validity of the developed model has been checked against an experimental study [2] conducted at the Institute of Technical Thermodynamic, Aachen – Germany, where this simulation study has been carried out. The complex experimental rig has been built to investigate the water vapor uptake of zeolite layers of defined cylindrical dimensions. The results of the experimental investigation and the numerical simulation show a very good fit with a maximum error of approximately 4%.

INTRODUCTION

Adsorption of vapor and gases into an adsorbent has obtained an increased and significant importance in the area of environmental protection in recent years. In the last three decades, the technical applications of the adsorption processes have shown a remarkable progress.

Adsorption heat pumps make use of the low temperature waste energy, which otherwise would be lost to the surroundings, instead of high-energy fuels. Use of waste energy serves to save energy in addition to avoiding of environmental pollution that would arise from the burning of high-energy fuels. The adsorption heat pumps employ, for example, the non-poisonous, non-flammable and minimally corrosive working pairs of zeolite and water [3].

The rate of adsorption in porous adsorbents is controlled by heat and mass transport phenomena

within the pore network [4]. The determination of the heat and mass transfer rates in adsorbents is, therefore, an important prerequisite in the optimization of heat pumps. The adsorption of water-vapor into a porous solid adsorbent such as zeolite can be described by the following three processes:

1. Breaking-up of the mass transport resistance at the boundary of the porous particle;
2. Diffusion in the adsorbent particle and
3. Adsorption at the inner surface of the particle, release of heat of sorption and temperature rise within the particle.

The heat of sorption developed within the particle has to be removed from the particle by conduction and then given up to a cooling medium at the surface by convection [5-6], to increase water-vapor uptake capacity of the adsorbent. The rate at which gaseous molecules are adsorbed by the adsorbent depends not only on the mass transfer mechanism but also on the temperature profile within the adsorbent. Due to the heat of sorption generated, the temperature of the adsorbent particle rises, which reduces its water vapor uptake capacity. Further mass transport into the adsorbent particle is then possible only when this heat of sorption is removed.

Based on certain assumptions, analytical solutions for the heat and mass transfer in porous medium have been obtained [7-8]. To solve the cumbersome expressions involved, even for the simple equilibrium relation, linear relations are assumed for the analytical solutions [7]. Adsorption in spherical particles have been analysed with diffusion taken as the sole factor in the process [9-10]. In these analyses the *Fourier series expansion* and the *penetration theory* have been implemented for the solution. Studies of one-dimensional analysis of non-isothermal adsorption processes have also been presented [11-12]. In the analyses, the assumption of isothermal adsorption has been disqualified, particularly for large adsorption rates. Recently, two new rate models – the *modified shell*

core (MSC) and the general driving force (GDF) models has been analysed in which the Fourier series expansion method have been integrated in the analytical solution [13]. The various studies indicated above have analysed one-dimensional heat and mass transfer in porous media. A three-dimensional, non-equilibrium model has been developed only very recently, in which the linear driving force (LDF) equation has been used to describe the mass transfer resistance within the pores particles while Darcy's law has been applied to describe the flow of adsorbate within the inter-particles [14].

The present study is carried out to investigate the kinetics of heat and mass transfer and adsorption dynamics in a two-dimensional cylindrical zeolite adsorber. The two-dimensional zeolite adsorber is numerically simulated by solving the energy and continuity equations considering the diffusive enthalpy rate of flow of the adsorbed vapor using the gPROMS program [1], with the necessary initial and boundary conditions specified. The simulation outputs are then compared with experimental results rendering an excellent fit, validating the model.

PHYSICAL MODEL

A schematic diagram of an adsorber segment with a single cylindrical zeolite layer placed on the annular fin is shown in Fig. 1. Heat of sorption generated within the zeolite layer is first conducted to the metal fin and then given out to the stream of water flowing through the tube.

MATHEMATICAL MODEL

Considering the effect of the diffusive enthalpy rate of absorbed gas, a new form of energy equation has been derived in the Cartesian coordinates [15]. Following the same analogy, the energy equation in cylindrical coordinates has been derived as given below.

Energy Equation:

$$\frac{\partial}{\partial t}(\rho U) = \frac{\partial}{\partial z} \left(\lambda_z \frac{\partial T}{\partial z} \right) + \frac{1}{r} \frac{\partial}{\partial r} \left(\lambda_r \frac{\partial T}{\partial r} \right) + \frac{1}{r^2} \frac{\partial}{\partial \theta} \left(\lambda_\theta \frac{\partial T}{\partial \theta} \right) - \frac{\partial}{\partial z} (m''_z h_z) - \frac{1}{r} \frac{\partial}{\partial r} (r m''_r h_r) - \frac{1}{r} \frac{\partial}{\partial \theta} (m''_\theta h_\theta) \quad (1)$$

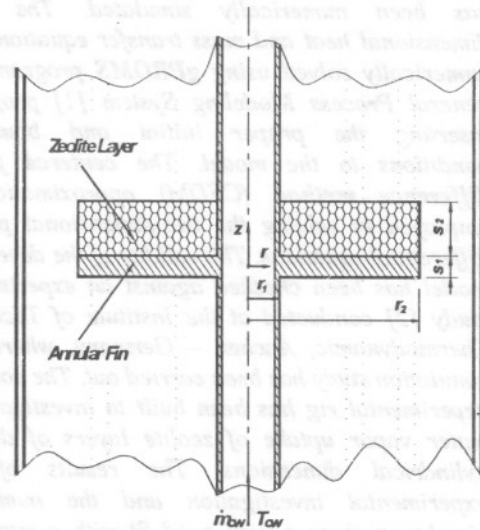


Fig. 1 Physical Model with a Single Cylindrical Zeolite Layer

U is the specific internal energy of wetted zeolite and is a function of both the water uptake and the prevailing temperature [16].

Continuity Equation:

$$\frac{\partial \rho}{\partial t} = - \frac{\partial}{\partial z} (m''_z) - \frac{1}{r} \frac{\partial}{\partial r} (r \cdot m''_r) - \frac{1}{r} \frac{\partial}{\partial \theta} (m''_\theta) \quad (2)$$

The following basic assumptions have been considered in solving the combined energy and continuity equations.

1. The heat and mass transfer processes are considered to be transient and two dimensional (r, z) .
2. All phases within an infinitesimally small zeolite sub-layer remain in a thermodynamic equilibrium whereby the water-vapor uptake in one element can be determined at the equilibrium isotherm.

3. The heat content within the vapor phase can be neglected for the density ratio between vapor and liquid phase is very small. At the working temperature and pressure of 100 °C and 100 mbar respectively, for example, the density ratio between vapor and liquid is approximately 5×10^{-5} .
4. The zeolite layer and the adsorbed water are considered incompressible.
5. The mass transfer within the zeolite layer is determined from the macropore diffusion of water vapor. The diffusion of adsorbed water through the zeolite walls are negligibly small [5].

Mass Transfer:

The mass flow rates of adsorbent in the radial and axial directions per unit area, given in Eqs. (1) and (2) are defined as:

$$\left. \begin{aligned} m''_r &= \frac{m_r}{A} \\ m''_z &= \frac{m_z}{A} \end{aligned} \right\} \quad (3)$$

The heat transfer within the zeolite crystal is expressed in terms of the effective thermal conductivity λ_{zoo} which takes the porosity of the zeolite particles ψ_{MaP} into account and is given by:

$$\lambda_{zoo} = \lambda_c \cdot (1 - \psi_{MaP}) \quad (4)$$

where $\lambda_c = 0.58 \text{ W/(m K)}$ [5] and $\psi_{MaP} = 0.55$ [3].

Neglecting the volume of the charged water-vapor content in the zeolite particle, the density may be expressed as [17]:

$$\rho = \rho_{zoo} \cdot (1 + x); \quad (5)$$

where ρ_{zoo} is the density of the zeolite crystal.

From Eq. (5), the quantity of water-vapor charged into a zeolite particle per kg of dry zeolite as a function of its coordinates is:

$$x(r, z) = \frac{\rho(r, z)}{\rho_{zoo}} - 1; \quad \begin{cases} z \in [0, s_2] \\ r \in [r_1, r_2] \end{cases} \quad (6)$$

In the model, the tube and water flowing through it are considered as a lumped system. The temperature distribution and consequently heat transfer within the fin are determined by solving the energy equation, Eq. (1), after omitting the last 4 terms and substituting the appropriate properties of the fin material.

Initial conditions:

Initially, both the fin and the zeolite layer are assumed to be at the temperature of the water vapor.

$$T_{fin}(r, z) = T_v; \quad \begin{cases} z \in [0, s_1] \\ r \in [r_1, r_2] \end{cases} \quad (7)$$

$$T_{zoo}(r, z) = T_v; \quad \begin{cases} z \in [0, s_2] \\ r \in [r_1, r_2] \end{cases} \quad (8)$$

Boundary conditions:

- During the absorption process heat is generated within the zeolite particles. Heat generated at the surface of the zeolite layer tends to heat up water vapor molecules at its vicinity. However, as these water vapor molecules are consequently adsorbed into the surface, heat transfer from the upper as well as the outer radius zeolite layer to the vapor phase at the interface can be neglected [18].
- For the mass transfer within the zeolite layer, it is assumed that the pressure is equal to the locally prevailing pressure.
- **Fin:**
 1. The lower surface of the fin is at the same temperature of as the water vapor temperature.

$$\frac{\partial T_{fin}(r, 0)}{\partial s} = 0; \quad \begin{cases} s_1 = 0 \\ r \in (r_1, r_2) \end{cases} \quad (9)$$

2. There is no heat transfer from the outer radius of the fin towards the water vapor and vice-versa.

$$\frac{\partial T_{fin}(r_2, z)}{\partial r} = 0; \quad z \in [0, s_1] \quad (10)$$

3. Heat transfer from the inner radius of the fin to the tube:

$$\lambda_{fin} \frac{\partial T_{fin}(r_1, z)}{\partial r} = \alpha_{cw} [T_{fin}(r, z) - T_{cw}]; \quad z \in [0, s_1] \quad (11)$$

• **Zeolite layer:**

1. There is no heat transfer from the inner radius of the zeolite layer to the tube:

$$\frac{\partial T_{zeo}(r_1, z)}{\partial r} = 0; \quad z \in [0, s_2] \quad (12)$$

2. There is no heat flow from the outer radius of the zeolite layer to the water vapor.

$$\frac{\partial T_{zeo}(r_2, z)}{\partial r} = 0; \quad z \in [0, s_2] \quad (13)$$

Connecting conditions:

At the junction between the upper surface of the fin and the lower surface of the zeolite layer, the following connecting equation is considered.

$$\lambda_{fin} \frac{\partial T_{fin}(r, s_1)}{\partial s_1} = \lambda_{zeo} \frac{\partial T_{zeo}(r, 0)}{\partial s_2}; \quad r \in [r_1, r_2] \quad (14)$$

The percentage of water charged, in a decimal form, is described by the relative water content as:

$$\chi = \frac{x_{ave} - x_0}{x_{\infty} - x_0} \quad (15)$$

which is the ratio of the actual quantity of water adsorbed to the maximum possible adsorption. The

average water uptake x_{ave} , in Eq. (15), is the integrated water vapor uptake divided by the area of the particular layer. In order to compare the computed results with the experimental data, which are the average values of water vapor uptake and pressure, the calculated values have to be averaged over the whole domain.

The time rate of decrease of the mass of water vapor in the vapor phase is equal to the sum of the integrated mass flow rates of the adsorbed water in the axial and radial directions of the zeolite layer, \dot{m}_{v_ads} .

$$\frac{\partial m_v}{\partial t} = - \dot{m}_{v_ads} \quad (16)$$

where the mass of water m_v is determined at the prevailing conditions, assuming that the water vapor behaves as ideal gas:

$$m_v = \frac{p_v \cdot V}{R \cdot T_v} \quad (17)$$

SOLUTION METHOD

For the very fact that periodically operating adsorption heat pumps work under transient conditions, the energy and continuity equations, considering the diffusion enthalpy rate of the adsorbed water, expressed above, are co-ordinate and time dependent. To consider the coordinate dependency of properties, the fin and the zeolite layers are separately discretised into balance elements in both the radial and axial directions. Within each of the balance elements, there exists a state of homogeneity with time dependent properties. Proper definition of the computational model allows the coupling of the adjoining balance elements with each other in the determination of combined heat and mass transfer.

The gPROMS program has been implemented as a device for the system simulation. The advantage of using this program over other simulation programs is its power of direct conversion, without the need of simplifying the partial differential equations, to the set algebraic equations. The system of differential equations is automatically discretised, converted into simple system of differential algebraic equations, handled by the built in routines, and numerically solved.

For the simulation process, an Input-File is prepared in which the actual problem is modeled. The created Input-File is then called by gPROMS, read, transformed and its syntax free characteristic verified. At the end, processes defined in the Input-File will be at disposition for execution. In solving the partial differential equations, gPROMS uses the line method approach [19] in which the solution function is parameterized such that it becomes dependent on a continuous co-ordinate, at least on time.

In this paper, among the various discretisation techniques for the approximation of the partial differential equations to algebraic equations available within gPROMS, the centered finite difference method (CFDM) is applied.

RESULTS

For the purpose of comparison of the dynamics of heat and mass transfer during the adsorption process, data taken from experimental investigation [17] carried out at the same institute where this study has been conducted have been implemented.

The relevant data taken from the experimental studies and used in the current simulation process are given in Table 1. In checking the validity of the set of heat and mass transfer equations and initial conditions prevailing for the physical model given exchanger, the temperature of which is maintained constant. The adsorber is connected to the vapor tank at time $t=0$, via a valve.

Table 1. State Variables and Geometric Data of Experimental Investigation

Initial water content	$x_0 = 0.149$ [kg w/kg zeo]
Final water content	$x_\infty = 0.169$ [kg w/kg zeo]
Initial pressure	$p_0 = 7.5$ [mbar]
Final pressure	$p_v = 16.4$ [mbar]
Wall temperature	$T_w = 96$ [°C]
Zeolite mass (dried)	$m_{zeo} = 3.86$ [g]
Volume of water-vapor container	$V_{Tank} = 23.5$ [l]

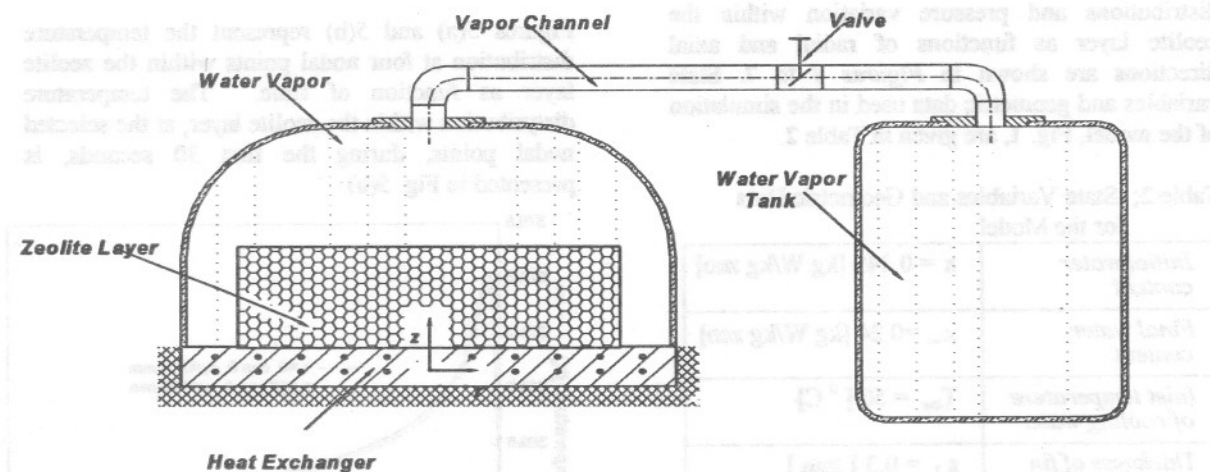


Fig. 2 A Simplified Experimental Setup for the Investigation of Water-Vapor Uptake

in Fig 1, only the boundary conditions are modified to match the conditions of the experimental set-up.

A simplified schematic diagram of the complex experimental investigation rig, [2], [3], is indicated in Fig. 2. The zeolite layer is fixed on to a heat

Figure 3 shows the experimental and computed results of the relative water content as a function of time, with data for the computational analysis taken from experimental studies, Table 1. The results obtained from simulation are in an excellent agreement with the experimental results, with a maximum relative error of approximately 4%. This is a clear indication of the applicability of the

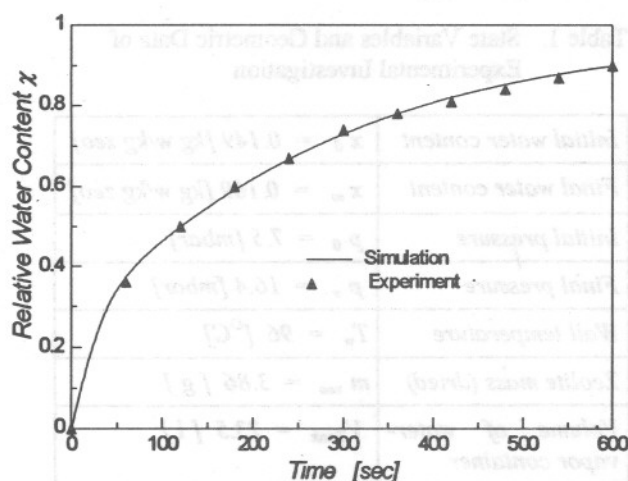


Fig. 3 Experimental and Simulation Results of Relative Water Content presented model in the optimization and determination of the combined heat and mass transfer dynamics in zeolite adsorbent.

The transient temperature distribution within the fin and the temperature and concentration distributions and pressure variation within the zeolite layer as functions of radial and axial directions are shown in Figures 4 to 7. State variables and geometric data used in the simulation of the model, Fig. 1, are given in Table 2.

Table 2; State Variables and Geometric Data for the Model

Initial water content	$x = 0.149$ [kg W/kg zeo]
Final water content	$x_{\infty} = 0.24$ [kg W/kg zeo]
Inlet temperature of cooling water	$T_{cw} = 50$ [$^{\circ}$ C]
Thickness of fin	$s_1 = 0.3$ [mm]
Thickness of zeolite layer	$s_2 = 1$ [mm]
Inner radius of zeolite layer/fin	$r_1 = 9$ [mm]
Outer radius of zeolite layer/fin	$r_2 = 16$ [mm]

For the determination of the temperature distribution within the fin as well as the zeolite layer and the pressure distribution and consequently the concentration distribution within the zeolite layer, the fin and the zeolite layers are discretized. The fin of 0.3 mm thickness and radius of ($r_2 - r_1$) of 7 mm is discretized into 6 steps in the axial direction and 20 steps in the radial direction, forming 120 nodal points. On the other hand, the zeolite layer of thickness 4 mm and radius of 7 mm is discretized into 20 steps in the axial direction and 20 steps in the radial direction, forming 400 nodal points.

Temperature Distribution:

Transient temperature distributions within the fin at two nodal points are shown in Fig. 4. Nodal points selected for representing the temperature distribution within the fin are at $r = r_1$ and $r = r_2$ in the radial direction and at half the thickness of the fin (that is at $z = 0.5s_1$) in the axial direction.

The heat of sorption generated within the zeolite layer and which is conducted to the fin heats up the layer at the start of the process. As this conducted heat is transferred to the cooling water, the temperature within the fin drops gradually. At the closest node to the tube, cooling starts earlier than the furthest node resulting in lower peak temperature.

Figures 5(a) and 5(b) represent the temperature distribution at four nodal points within the zeolite layer as function of time. The temperature distribution within the zeolite layer, at the selected nodal points, during the first 30 seconds, is presented in Fig. 5(b).

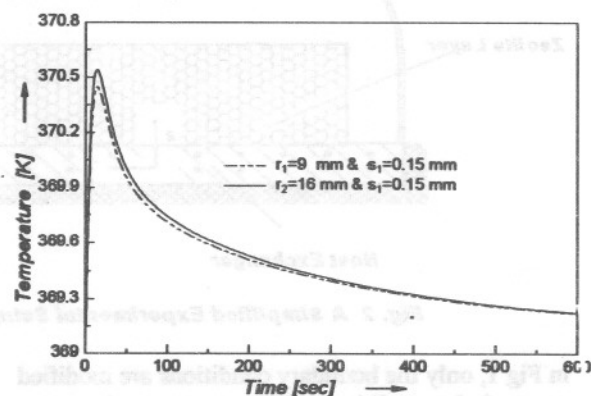


Fig. 4 Temperature Distribution within Fin

The selected nodal points are the intersection points of $r = r_1 + 2x\Delta r$ and $r = r_2 - 2x\Delta r$ and $z = 5x\Delta s_2$ and $z = 15x\Delta s_2$. The average temperature T_{ave} for the entire layer is also shown as function of time. At the beginning of the adsorption process, the zeolite layer at the furthest point from the fin gets heated up faster. As heat is conducted through the layers towards the fin, the temperature of zeolite layer closer to the fin gradually gets higher. Heat of conduction from layers further from the fin towards layers closer to the fin and consequent transfer of heat to the fin and eventually to the cooling water causes a gradual temperature drop as indicated in Fig. 5 (a).

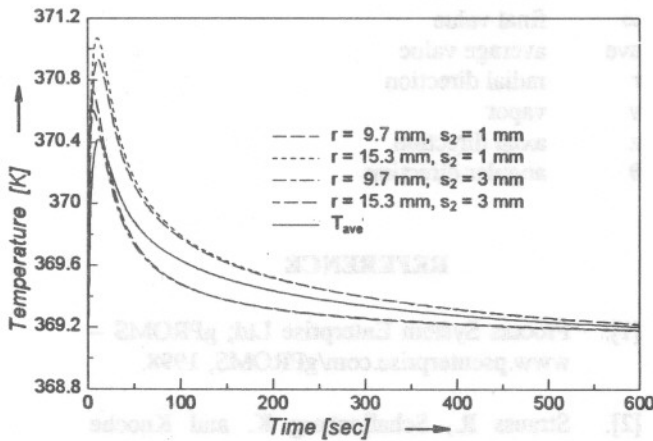


Fig. 5(a) Temperature Distribution within Zeolite Layer

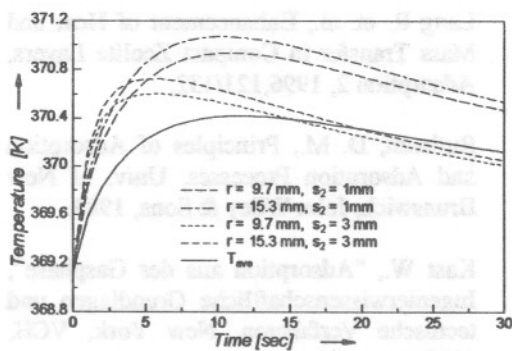


Fig. 5(b) Temperature Distribution within Zeolite Layer

Pressure Distribution:

Pressure distribution within the zeolite layer at six nodal points as function of time, are indicated in Fig. 6. Nodal points at the intersections of $r = r_1 + 2x\Delta r$ & $r = r_2 - 2x\Delta r$ and $z = 5x\Delta s_2$, $z = 10x\Delta s_2$ & $z = 15x\Delta s_2$ are selected in representing the pressure

(concentration) distribution. The further the zeolite layer from fin, the higher is the prevailing pressure.

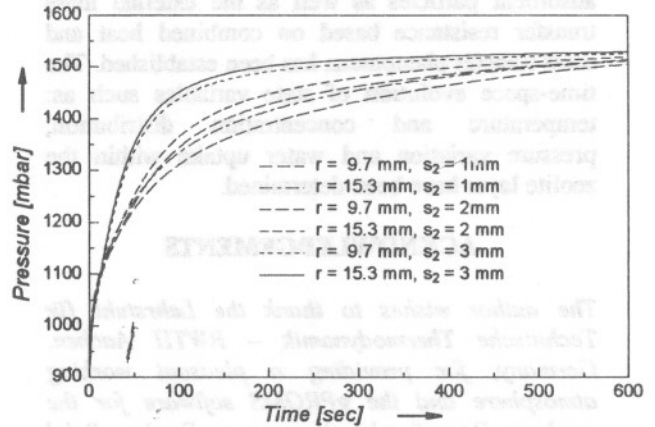


Fig. 6 Pressure Distribution within Zeolite Layer

Water Vapor Uptake:

Water-uptake within the zeolite is presented at the same nodal points chosen for describing the pressure distribution in Fig. 6. The water uptake Fig. 7 follows the same trend as the prevailing pressures within zeolite layer.

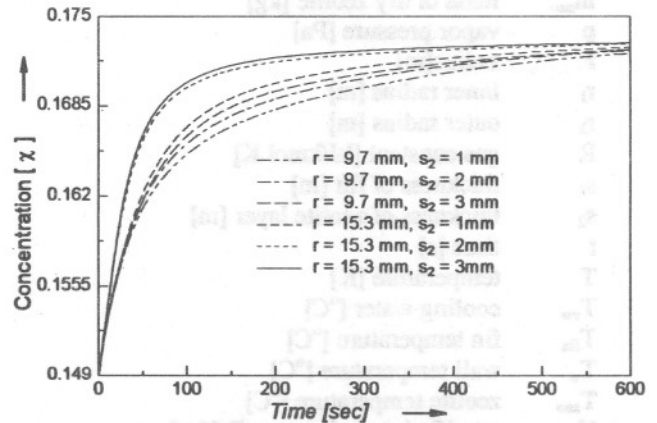


Fig. 7 Concentration Distribution within Zeolite Layer

For the considered state variables of the analysis, the rate of water-vapor charged into the zeolite layer is higher during the first 600 seconds.

CONCLUSION

A transient two-dimensional model, which takes into account the adsorption kinetics inside adsorbent particles as well as the external mass transfer resistance based on combined heat and mass transfer phenomena has been established. The time-space evolution of state variables such as: temperature and concentration distribution, pressure variation and water uptake within the zeolite layer have been determined.

ACKNOWLEDGEMENTS

The author wishes to thank the Lehrstuhl für Technische Thermodynamik – RWTH Aachen, Germany, for providing a pleasant working atmosphere and the gPROMS software for the analysis. Deep thanks also goes to Dr.-Ing. Belal Dawoud for the numerous technical discussions conducted during this work. The study period at the Lehrstuhl für Technische Thermodynamik has been sponsored by the German Academic Exchange Service (DAAD) and is gratefully acknowledged.

Nomenclature

A	area [m ²]
\dot{m}	mass flow rate [kg/s]
\dot{m}	mass flow rate per unit area [kg/(s m ²)]
m_{zeo}	mass of dry zeolite [kg]
p	vapor pressure [Pa]
r	radius [m]
r_1	inner radius [m]
r_2	outer radius [m]
R	gas constant [kJ/kmol K]
s_1	thickness of fin [m]
s_2	thickness of zeolite layer [m]
t	time [s]
T	temperature [K]
T_{cw}	cooling water [°C]
T_{fin}	fin temperature [°C]
T_w	wall temperature [°C]
T_{zeo}	zeolite temperature [°C]
U	specific internal energy [kJ/kg]
V_{Tank}	Volume of vapor tank [m ³]
x	adsorbed quantity of water [-]
Δr	fin/zeolite thickness of a single step in radial direction [m]
Δs_1	fin thickness of a single step in axial direction [m]

Δs_2	zeolite thickness of a single step in axial direction [m]
α_{cw}	heat transfer coefficient of cooling water [W/m ² K]
λ	thermal conductivity [W/m K]
λ_x	thermal conductivity of zeolite crystal [W/m K]
ρ	density [kg/m ³]
Ψ_{MaP}	porosity of zeolite [-]
χ	relative water content [-]

Subscripts:

0	initial value
∞	final value
ave	average value
r	radial direction
v	vapor
z	axial direction
θ	angular direction

REFERENCE

- [1]. Process System Enterprise Ltd; gPROMS – www.psenterprise.com/gPROMS, 1998.
- [2]. Strauss R., Schallenberg K. and Knoche K.F., Measurement of Kinetics of Water Vapor Adsorption into Zeolite Layers, 1992.
- [3]. Lang R. et al., Enhancement of Heat and Mass Transfer in Compact Zeolite Layers, Adsorption 2, 1996, 121/132.
- [4]. Ruthven, D. M., Principles of Adsorption and Adsorption Processes, Univ. of New Brunswick, John Wiley & Sons, 1984.
- [5]. Kast W., "Adsorption aus der Gasphase", Ingenieurwissenschaftliche Grundlagen und technische Verfahrenen, New York, VCH, 1988.
- [6]. Brunovska A. et Al., Chemical Engineering Science, 33, 1978.
- [7]. Rosen J.B., Ind. Engng. Chem. Fundamentals, 46, 1954.

- [8]. Masamune S. and Smith J.M., Ind. Engng. Chem. Fundamentals, 3, 1964.
- [9]. Carta Giorgio, The Linear Driving Force Approximation for Cyclic Mass Transfer in Spherical Particles, Chemical Engineering Science,48,1991.
- [10]. Scott D. M., The Linear Driving Force Model of Cyclic Adsorption and Desorption: The Effect of Shape, Chemical Engineering Science,49,1994.
- [11]. Brunovska A. et. al., Analysis of A Non-isothermal One-Component Sorption in a Single Adsorbent Particle, Chemical Engineering Science,33,1978.
- [12]. Brunovska A. et. al., Analysis of A Non-isothermal One-Component Sorption in a Single Adsorbent Particle – A Simplified Model, Chemical Engineering Science,36,1981.
- [13]. Yao C. and Tien C., Application of New Rate Models to Cyclic Adsorption in Adsorbents, Chemical Engineering Science,53,1998.
- [14]. Zang L.Z. and Wang L., Momentum and Heat Transfer in the Adsorbent of a Waste-Heat Adsorption Cooling System,Energy, 24,1999.
- [15]. Knoche K. F. , Technische Thermodynamic – Teil 2. – 6.Edition, Darmstadt, 1997.
- [16]. Dawoud B., Thermische und Kalorische Stoffdaten des Stoffsystems Zeolith MgNaA-Wasser, Dissertation, RWTH-Aachen,1999.
- [17]. Gerlich A., Gekoppelter Wärme- und Stofftransport in der kompakten Zeolithschicht einer Adsorptionswärmepumpe, Dissertation, RWTH-Aachen 1993.
- [18]. Westerfeld T., Numerische Untersuchung einer periodisch arbeitenden Adsorptionswärmepumpe, Dissertation, RWTH-Aachen,1996.
- [19]. Schiesser W. F., The Numerical Method of Lines, Academic Press, New York, 1991.